

Optical switching of electron transport in a waveguide-QED system

Nzar Rauf Abdullah,^{1,2,*} Chi-Shung Tang,³ Andrei Manolescu,⁴ and Vidar Gudmundsson²

¹*Physics Department, Faculty of Science and Science Education,
School of Science, University of Sulaimani, Kurdistan Region, Iraq*

²*Science Institute, University of Iceland, Dunhaga 3, IS-107 Reykjavik, Iceland*

³*Department of Mechanical Engineering, National United University, 1, Lienda, Miaoli 36063, Taiwan*

⁴*Reykjavik University, School of Science and Engineering, Menntavegur 1, IS-101 Reykjavik, Iceland*

Electron switching in waveguides coupled to a photon cavity is found to be strongly influenced by the photon energy and polarization. Therefore, the charge dynamics in the system is investigated in two different regimes, for off- and on-resonant photon fields. In the off-resonant photon field, the photon energy is smaller than the energy spacing between the first two lowest subbands of the waveguide system, the charge splits between the waveguides implementing a $\sqrt{\text{NOT}}$ -quantum logic gate action. In the on-resonant photon field, the charge is totally switched from one waveguide to the other due to the appearance of photon replica states of the first subband in the second subband region instigating a quantum-NOT transition. In addition, the importance of the photon polarization to control the charge motion in the waveguide system is demonstrated. The idea of charge switching in electronic circuits may serve to built quantum bits.

PACS numbers: 42.50.Pq, 73.21.Hb, 03.65.Yz, 05.60.Gg, 85.35.Ds

I. INTRODUCTION

Quantum information processing is a rapidly growing field promising to harness the laws of quantum physics for the sake of improvements in computer technology [1]. One of the exciting aspects of the quantum information processing is the development of effective and fast computation strategies for data manipulation with many possibilities [2]. A number of different quantum systems are being explored to implement a quantum bit (qubit) [3–5]. Among these, double waveguides represented by a double quantum wire is a candidate to build a qubit. A coupling element called coupling window is put between the waveguides to allow for inter-waveguide transport [4]. In this system, the length of the coupling window can be tuned to form the proposed qubit and implement quantum logic gates [6]. Ionicioiu et al. have suggested the same scheme for quantum computation. In their scheme, a single electron is transported through a double quantum waveguide which states can be represented as qubit state $|1\rangle$ and $|0\rangle$ [7]. The manipulation of $|0\rangle$ to $|1\rangle$ or vice versa is performed by a quantum gate. The quantum NOT operation just negates the logical value: 0 becomes 1, and 1 becomes 0. In addition, the superposition of 0 and 1 forms the $\sqrt{\text{NOT}}$ quantum logic gate action. Several methods such as magnetic switching [8], electrically tunable [9], and split-gate method [10] have been used as a quantum gate to implement quantum logic actions in double waveguide system.

Recently, we investigated approaches to switch electron motion between two waveguides by a split-gate method, magnetic field, and photon cavity. In addition, we reported the importance of the Coulomb interaction in

the electron switching [11, 12]. In this work, we investigate the processes of electron switching in a coupled waveguide where a window coupling is placed between the waveguides. Our approach here is to use a single-photon mode to manipulate the electron motion between the two waveguides in two regimes, for off- and resonant photon field. The transient electron transport in the waveguide system is described using a generalized master equation [13, 14]. The switching processes implement the quantum logic gate actions in the double waveguide system representing the quantum bit.

This paper is organized as following: In Sec. II we define the model and theoretical methods. The results and conclusions are presented in Sec. III and Sec. IV, respectively.

II. MODEL AND THEORY

In this section, the model under investigation is introduced. We assume two symmetric waveguide system weakly coupled to two electron reservoirs or leads shown in Fig. 1. The bottom- and top-waveguide are so called control- and target-waveguide, respectively. The waveguides are coupled via a coupling element called the coupling window that allows inter waveguide transport and electron interference between the waveguides. The control-waveguide is coupled to a lead from the left side and both waveguides are connected to a lead from right side.

The waveguide system is hard-wall confined in the x -direction and parabolically confined in the y -direction. The waveguide potential can be described by

$$U_{\text{WG}}(r) = U_0 \left[-e^{(-\alpha_0^2 x^2)} + e^{(-[\alpha_x^2 x^2 + \alpha_y^2 y^2])} \right]. \quad (1)$$

Herein, U_0 is the strength of the confinement potential, and α_0 , α_x and α_y are constants. The first term describes

* nzar.r.abdullah@gmail.com

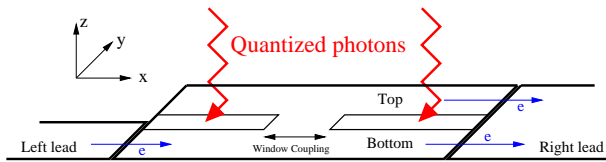


FIG. 1. (Color online) Schematic diagram shows two coupled waveguides connected to two leads. The bottom waveguide is coupled to the left and the right leads while the top waveguide is only connected to the right lead. Here, top and bottom refers to the y -direction. The coupling window allows inter-waveguide transport. The photon field is represented by red zigzag arrows and the blue arrows indicate the direction of electron motion in the system.

the potential barrier between the waveguides and the second is their coupling potential, or coupling window.

The waveguide system is placed in a rectangular photon cavity with the cavity much larger than the waveguide system. The cavity contains a single photon mode and the photons are linearly polarized in the cavity either parallel or perpendicular to the direction of the electron motion in the waveguide system. The Hamiltonian of the double waveguide system coupled to a single photon mode in an external perpendicular magnetic field in the z -direction is [15, 16]

$$\hat{H} = \int d^2r \hat{\psi}^\dagger(\mathbf{r}) \left[\frac{\hat{\mathbf{P}}^2}{2m^*} + U_{\text{WG}}(\mathbf{r}) \right] \hat{\psi}(\mathbf{r}) + \hat{H}_C + \hat{H}_\gamma, \quad (2)$$

where $\hat{\psi}$ is the field operator, m^* indicates the effective mass of an electron, and the canonical momentum operator is described as

$$\hat{\mathbf{P}} = \left(\frac{\hbar}{i} \nabla + \frac{e}{c} \left[\hat{\mathbf{A}}(\mathbf{r}) + \hat{\mathbf{A}}_\gamma(\mathbf{r}) \right] \right). \quad (3)$$

Herein, $\hat{\mathbf{A}}(\mathbf{r}) = -By\hat{x}$ is the vector potential of the external constant magnetic field defined in the Landau gauge, and $\hat{\mathbf{A}}_\gamma$ is the photonic vector potential of the cavity given by $\hat{\mathbf{A}}_\gamma(\mathbf{r}) = A(\hat{a} + \hat{a}^\dagger)\mathbf{e}$, with A the amplitude of the photon field, $g_\gamma = eAa_w\Omega_w/c$ the electron-photon coupling constant, $\mathbf{e} = \mathbf{e}_x$ for a longitudinally-polarized photon field (TE₀₁₁), or $\mathbf{e} = \mathbf{e}_y$ for transversely-polarized photon field (TE₁₀₁), and $\hat{a}(\hat{a}^\dagger)$ are annihilation(creation) operators of the photons, respectively. The effective confinement frequency is $\Omega_w = \sqrt{\Omega_0^2 + \omega_c^2}$ with Ω_0 the electron confinement frequency due to the lateral parabolic potential and ω_c the cyclotron frequency due to external magnetic field. The confinement frequency defines a natural length scale $a_w = \sqrt{\hbar/(m^*\Omega_w)}$, the effective magnetic length. The second term of Eq. (2) (\hat{H}_C) is the Coulomb interaction between the electrons in the waveguide system [17]. The last term of Eq. (2) represents the quantized photon field $\hat{H}_\gamma = \hbar\omega_\gamma\hat{a}^\dagger\hat{a}$ with $\hbar\omega_\gamma$ the photon energy. We investigate the electron transport properties in the waveguide-cavity system in the case of off- and on-resonant pho-

ton fields including both the para- and the diamagnetic electron-photon interactions without the rotating wave approximation [16]. The electron-electron and the electron-photon interactions are treated by exact diagonalization.

The waveguide system is coupled to external leads as indicated in Fig. 1 and described in earlier work [11, 12]. The left and right leads are coupled simultaneously smoothly within 20 ps to the waveguide system by the use of switching functions [13].

We consider the leads to be held at the same temperature T , and their overall coupling strength to the waveguides is $g_{\text{LR}}a_w^{3/2}$.

The continuous spectrum of the states in the leads which are treated as electron reservoirs, make the solution of the Liouville-von Neumann equation for the time evolution of the whole system impractical. Instead, we use a formalism to project the time-evolution of the whole system onto the open system consisting of the waveguides and the cavity, transforming the Liouville-von Neumann equation for the full density operator to a generalized non-Markovian master equation for the reduced density operator (RDO) [18, 19]. This operation introduces complicated dissipation terms into the equation of motion describing the loss or gain of electrons and energy from the leads. The master equation describes the time-evolution of the RDO for the open waveguide system under the influences of the leads. The non-Markovian approach allows us to study the transient behavior of the system in the weak coupling of the leads to the waveguide system [13].

III. RESULTS

We consider two parallel waveguides made of a GaAs semiconductor material with electron effective mass $m^* = 0.067m_e$ and the relative dielectric constant $k = 12.4$. The waveguide system with length $L_x = 300$ nm is weakly coupled to two electron reservoirs. The transverse confinement energy of the electrons in the waveguide system is equal to that of the leads $\hbar\Omega_0 = \hbar\Omega_l = 1.0$ meV, where l stands for the left (L), or the right (R) lead. The temperature of the leads is assumed to be $T_l = 0.5$ K. The parameters that specify the potential barrier and the coupling window between the waveguide are $U_0 = 18.0$ meV, and $\alpha_0 = \alpha_y = 0.03$ nm⁻¹. The coupling window length is defined by $L_{\text{CL}} = 2/\alpha_x$, and $g_{\text{LR}}a_w^{3/2} = 0.5$ meV. In addition, we assume the cavity initially contains one photon.

A. Off-resonance photon field

In this section, we consider the photon energy smaller than the energy spacing between the first and the second subband of the waveguides. The system under this condition is in the so called off-resonance regime.

First, we show the results of the waveguide system without the photon cavity. Figure 2 shows the energy spectrum of the waveguide system with no electron-photon coupling. In Fig. 2(a) the many-electron (ME) energy versus the ME state $|\mu\rangle$ is plotted. The black lines indicate the chemical potential of the left (μ_L) and the right (μ_R) lead. It can be clearly seen that the first subband of the waveguide system is located in the bias window $\Delta\mu = \mu_L - \mu_R$ including six one-electron states. We can confirm that only four of them shown in the blue rectangle are active in the electron transport. The two lowest states, the ground state and the first-excited state, only weakly participate in the electron transport because of their electron localization property in the coupling window region. The four states are: second-, third-, fourth-, and fifth-excited states. The second subband contains six more states in the energy range 4.5-5.5 meV.

The coupling window between the waveguides can be varied to find a suitable coupling between the waveguides. Practically, the coupling window can be formed using 'finger' gates or a saddle potential [6]. In Fig. 2(b) the energy spectrum of the four active states shown in Fig. 2(a) versus the length of the coupling window is shown. We notice a crossing/anti-crossing (blue rectangle) in the energy spectrum occurring at length $L_{CL} = 40$ nm for the coupling window. The crossing point in the energy spectrum indicates a strong coupling or interference between the waveguides [20].

To illustrate the physical properties of electron transport in the crossing region, we display the net charge current and current density in the late transient regime at time $t = 200$ ps. Fig. 3 demonstrates the net charge current versus the coupling length for the waveguide system without (w/o) photon (ph) (blue lines) and with photon (w ph) cavity in the case of an x -polarized (red lines) and a y -polarized (green lines) photon field. The current is maximum at $L_{CL} = 40$ nm in the energy spectrum for the case of no electron-photon coupling (blue curve) corresponding to the crossing in the energy spectrum. The maximized current at 40 nm can be explained by observing charge current density. In a previous work, we have shown the dynamic motion of charge through the waveguide system in the absence of the Coulomb interaction [11] in which the incoming charge from the input bottom waveguide is equally split between the two outputs of the waveguides at $L_{CL} = 40$ nm. The splitting process of the charge density occurs due to a contribution of two electron states to the transport. But the Coulomb interaction breaks the splitting process by lifting the two electron states above the group of active states. Therefore, the charge density flows from the left lead to the right lead through the bottom waveguide without inter-waveguide backward or forward scattering as is shown in Fig. 4. The current is thus maximized and a current peak is seen for $L_{CL} = 40$ nm.

Now, we consider the waveguide to be embedded in the photon cavity. The photons are linearly polarized in either x or y -direction. As we mentioned above, the pho-

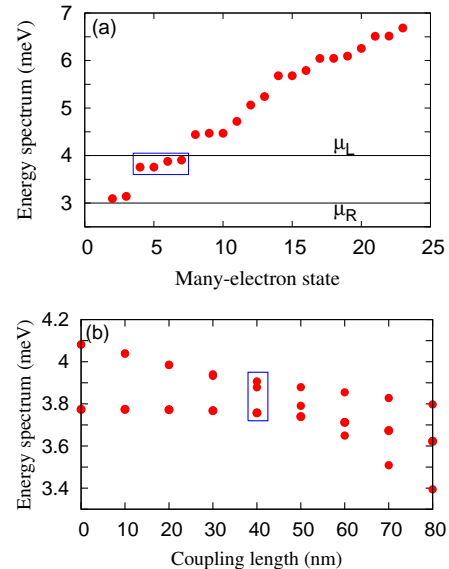


FIG. 2. (Color online) (a) Energy spectrum of the waveguide system versus many-electron state is plotted at $L_{CL} = 40$ nm. The black lines display the chemical potential of the left (μ_L) and the right (μ_R) lead. The states in the blue rectangle are active states in the transport. (b) Energy spectrum as a function of the coupling length in the case of no electron-photon coupling. The crossover in the energy spectrum shown in the blue rectangles indicates a proper coupling between the waveguides. The magnetic field is $B = 0.1$ T, $\hbar\Omega_0 = 1.0$ meV. The chemical potentials are $\mu_L = 3.0$ meV and $\mu_R = 4.0$ meV implying $\Delta\mu = 1.0$ meV.

ton energy is smaller than the energy spacing between the first and the second subband of the waveguide system. In the presence of the photon cavity, photon replica states are formed and they actively participate in the electron transport [12]. For the case of an off-resonant photon field we choose the energy $\hbar\Omega_\gamma = 0.5$ meV, which is smaller than the electron confinement energy of the waveguide system in the y -direction ($\hbar\Omega_0 = 1.0$ meV). In this case, the one-photon replicas of the four active states mentioned above are formed between the first and second subbands in the energy range [4.0-4.5] meV at $L_{CL} = 40$ nm. The participation of the photon replica states modifies the charge motion in the system. The dynamic motion of the charge at $L_{CL} = 40$ nm demonstrated in Fig. 5(a) indicates that it splits between the top and the bottom waveguides. The charge splitting here implements a quantum logic gate called a $\sqrt{\text{NOT}}$ -gate. This is analogue to the superposition of the ground state and excited state in a simple two level system in which the electron transmitted through both the $\langle 0|$ and the $\langle 1|$ states [21]. We notice that the current is decreased in the x -polarized case of the photon field as is shown in Fig. 3(a) (red lines).

Figure 5(b) displays the charge current density for the case of a y -polarized photon field. The charge is trans-

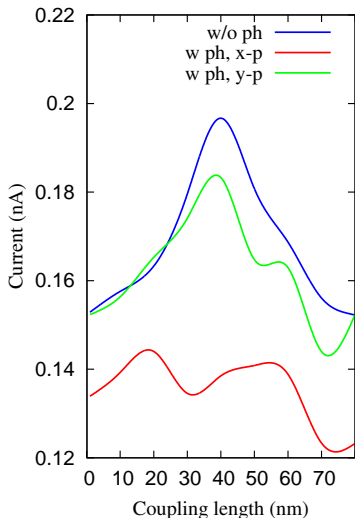


FIG. 3. (Color online) The net charge current versus coupling length of the waveguide system without (w/o) photon (ph) (blue lines) and with photon (w ph) cavity in the case of x -polarization (red lines) and y -polarization (green lines) of the photons in the case of the off-resonance photon field. The magnetic field is $B = 0.1$ T, $\hbar\Omega_0 = 1.0$ meV. The chemical potentials are $\mu_L = 3.0$ meV and $\mu_R = 4.0$ meV implying $\Delta\mu = 1.0$ meV.

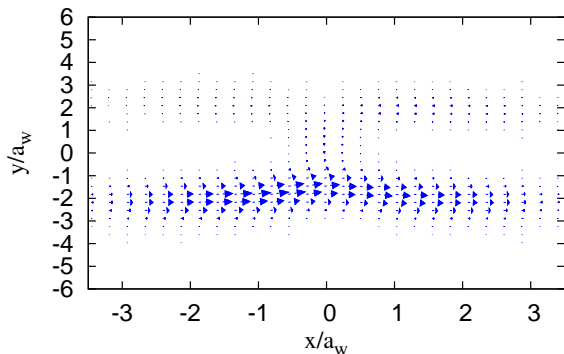


FIG. 4. (Color online) Charge current density in the waveguide system for the current peak at $t = 200$ ps and $L_{CL} = 40$ nm shown in Fig. 3 (blue lines). The electron-photon interaction is neglected here. The magnetic field is $B = 0.001$ T and the effective magnetic length is $a_w = 33.72$ nm.

ported through the bottom waveguide without much inter-waveguide transport. Consequently, the current of the peak is slightly decreased as is displayed in Fig. 3(a) (green lines).

The differing 'conductance' of the system with respect to the photon polarization reflects the geometric anisotropy of the waveguide system.

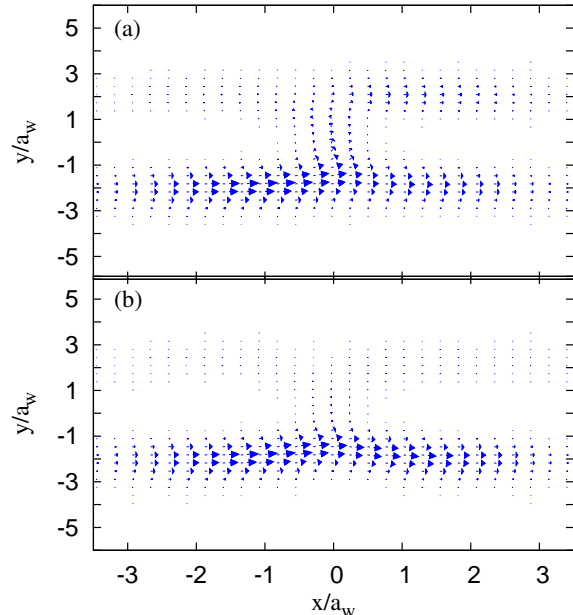


FIG. 5. (Color online) Charge current density in the waveguide system at $t = 200$ ps and $L_{CL} = 40$ nm for the system coupled to the photon cavity with x -polarization (a) and y -polarization (b) of the photon field corresponding to the current peak labeled as red line and green line shown in Fig. 3, respectively. The photon energy is $\hbar\omega_\gamma = 0.5$ meV and $g_\gamma = 0.1$ meV. The magnetic field is $B = 0.001$ T and the effective magnetic length is $a_w = 33.72$ nm.

B. Resonant photon field

In this section, we increase the photon energy to $\hbar\omega_\gamma = 0.7$ meV. However, the photon energy is still a bit smaller than the electron confinement energy of the waveguide system $\hbar\Omega_0 = 1.0$ meV, but we can obtain a total charge switching between the waveguides. The one photon replicas of the four active states mentioned in the previous section are now formed in the second subband when the photon energy is 0.7 meV. The second subband of the waveguide system becomes active in the electron transport. Consequently, the transmission of charge from the bottom guide input to the top guide output at $L_{CL} = 40$ nm is obtained in the x -polarized of the photon field as is shown in Fig. 6(a). The switching of the charge transport implements a NOT-operation quantum logic gate. But, for a y -polarized photon field presented in Fig. 6(b), the charge current is almost unchanged.

IV. CONCLUSIONS

The results achieved in this study lead to the conclusion that, by applying an optical source such as photons in a cavity to coupled waveguides, it is possible to stimulate electron switching between the two waveguides. A

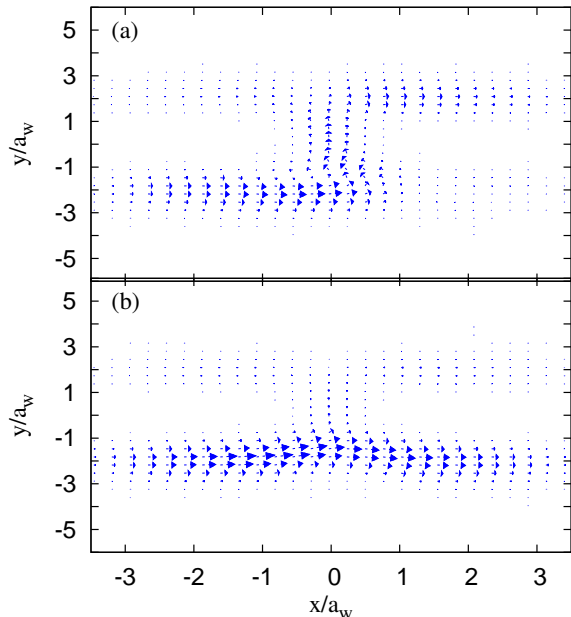


FIG. 6. (Color online) Charge current density in the waveguide system at $t = 200$ ps and $L_{CL} = 40$ nm for the system coupled to the photon cavity with x -polarization (a) and y -polarization (b) of the photon field. The photon energy is $\hbar\omega_\gamma = 0.7$ meV and $g_\gamma = 0.1$ meV. The magnetic field is $B = 0.001$ T and the effective magnetic length is $a_w = 33.72$ nm.

coherent propagation of an electron along a waveguide and a subsequent charge switching has been achieved. We initialize the double waveguide system by injecting a single electron in one of the waveguide, this is done by coupling one of the waveguides to a lead on the left side. Calculation of the final state is performed by coupling both waveguides to a lead on the right side. The length of the inter-waveguide coupling window is tuned leading

to a crossing point in the energy spectrum. The crossing indicates a strong coupling between the waveguides. The net charge current is thus at a maximum in the crossing region. By applying linearly polarized cavity photons to the electronic system in parallel quantum waveguides, we demonstrate the implementation of two types of quantum gates in the energy crossing region reflecting strong coupling of the waveguides. For an off-resonant x -polarized photon field, the splitting of the charge transfer has been found to be caused by a formation of photon replica states leading to a $\sqrt{\text{NOT}}$ -gate operation. For the on-resonant and x -polarized photon field, the charge transfer switches from one waveguide to the other. The motion of charge implements a NOT-operation quantum logic gate. We like to underline that the charge motion is not influenced by the photon field in the case of off- or on-resonance for the case of y -polarization due to the geometric anisotropy of the waveguide system. With this study we point out the possibility to use a waveguide-photon cavity system to implement the fundamental qubit operations needed for quantum information processing. Importantly, our time-dependent non-Markovian calculations point to the possibility to achieve the qubit switching in the late transient regime of the system.

ACKNOWLEDGMENTS

Financial support is acknowledged from the Icelandic Research and Instruments Funds, and the Research Fund of the University of Iceland. The calculations were carried out on the Nordic High Performance Computer Center in Iceland. We acknowledge the Nordic network NANOCONTROL, project No.: P-13053, University of Sulaimani, and the Ministry of Science and Technology, Taiwan through Contract No. MOST 103-2112-M-239-001-MY3.

-
- [1] M. Möttönen, J. J. Vartiainen, V. Bergholm, and M. M. Salomaa, *Phys. Rev. Lett.* **93**, 130502 (2004).
 - [2] M. G. Snyder and L. E. Reichl, *Phys. Rev. A* **70**, 052330 (2004).
 - [3] J. M. Martinis, S. Nam, J. Aumentado, and C. Urbina, *Phys. Rev. Lett.* **89**, 117901 (2002).
 - [4] A. Bertoni, P. Bordone, R. Brunetti, C. Jacoboni, and S. Reggiani, *Phys. Rev. Lett.* **84**, 5912 (2000).
 - [5] L. E. Reichl and M. G. Snyder, *Phys. Rev. A* **74**, 012318 (2006).
 - [6] A. Ramamoorthy, R. Akis, and J. P. Bird, *IEEE Transaction on nanotechnology* **5**, 712 (2006).
 - [7] R. Ionicioiu, G. Amaratunga, and F. Udrea, *Int. J. of Mod. Phys. B* **15**, 125 (2001).
 - [8] J. Harris, R. Akis, and D. K. Ferry, *Appl. Phys. Lett.* **79**, 2214 (2001).
 - [9] M. J. Gilbert, R. Akis, and D. K. Ferry, *Appl. Phys. Lett.* **81**, 4284 (2002).
 - [10] A. Ramamoorthy, J. P. Bird, and J. L. Reno, *Journal of Physics: Condensed Matter* **19**, 276205 (2007).
 - [11] N. R. Abdullah, C. S. Tang, A. Manolescu, and V. Gudmundsson, *Journal of physics: Condensed matter* **27**, 015301 (2015).
 - [12] N. R. Abdullah, C.-S. Tang, A. Manolescu, and V. Gudmundsson, *Journal of Applied Physics* **116**, 233104 (2014).
 - [13] V. Gudmundsson, O. Jonasson, T. Arnold, C.-S. Tang, H.-S. Goan, and A. Manolescu, *Fortschr. Phys.* **61**, 305 (2013).
 - [14] V. Moldoveanu, A. Manolescu, C.-S. Tang, and V. Gudmundsson, *Phys. Rev. B* **81**, 155442 (2010).
 - [15] T. Arnold, C.-S. Tang, A. Manolescu, and V. Gudmundsson, *Journal of Optics* **17**, 015201 (2015).

- [16] O. Jonasson, C.-S. Tang, H.-S. Goan, A. Manolescu, and V. Gudmundsson, *Phys. Rev. E* **86**, 046701 (2012).
- [17] N. R. Abdullah, C. S. Tang, A. Manolescu, and V. Gudmundsson, *Journal of Physics:Condensed Matter* **25**, 465302 (2013).
- [18] S. Nakajima, *Prog. of Theor. Phys.* **20**, 948 (1958).
- [19] R. Zwanzig, *The Journal of Chemical Physics* **33**, 1338 (1960).
- [20] T. Zibold, P. Vogl, and A. Bertoni, *Phys. Rev. B* **76**, 195301 (2007).
- [21] M. A. Nielsen and I. L. Chuang, *Quantum computation and Quantum Information* (Cambridge University Press, Cambridge, 2010).